Semiconductor Physics, Quantum Electronics & Optoelectronics. 2004. V. 7, N 3. P. 291-296.

PACS: 77.55.+f, 78.66.-w

Optical properties of dielectric layers with CeO_2

T.V. Semikina
Department of Environmental & Material Engineering, Teikyo University of Science & Technology,
2525 Yatsusawa, Uenohara-machi, Kitatsuru-gun, Yamanashi-pref., 409-0193 Japan,
E-mail: semikina@edd.ntu-kpi.kiev.ua, tanyasemikina@rambler.ru

Abstract. The polycrystalline thin films CeO_2, WO_3, amorphous complex films $WO_3 + CeO_2$ with content of CeO_2 in the powder 10, 15 and 20 %, and $CeO_2 + Dy_2O_3$ with content of Dy_2O_3 in the powder 10, 15 and 20 % are obtained by vacuum deposition method via powder evaporation. For the first time the optical characteristics of complex films $WO_3 + CeO_2$ and CeO_2+Dy_2O_3 are obtained. As a results of films investigation by ellipsometry the dependencies of refraction and extinction coefficients on incident beam energy are presented. The dielectric permittivity and energy band gapes are calculated. The refraction coefficients of films CeO_2 are 1.85–2.85 and are not more than 2.37 for complex films. Dielectric constant ε of complex films are 3.57–4.16, and ε =4.7 of CeO_2 film. The CeO_2, WO_3, and $WO_3 + CeO_2$ films have wide band gape E_g = 2.8–3.37 eV.

Keywords: oxide high-*k* materials, rare-earth elements, CeO_2, optical characteristics, dielectric permittivity, and wide band gap.

Paper received 22.05.04; accepted for publication 21.10.04.

1. Introduction

The ways of microelectronics development are based on a permanent decrease in integrated circuit component dimensions. For metal-oxide semiconductor field effect transistors (MOSFET), first of all, the gate length should be reduced, which consequently results in scaling all others dimensions and is accompanied by appearance of new technological problems [1,2]. Because of the dimension decrease, which is related with, reduction of the dielectric thickness under the gate, there appear such problems as a drop of the breakdown voltage of this layer, increase in leakage current and operation voltage values. SiO_2 is often used as a dielectric layer in silicon technology and certainly has excellent characteristics, namely: high quality of the interface between oxide silicon and silicon with density of surface traps ~10^{10} cm^{-2}eV^{-1}, breakdown voltage is 15 MV/cm, high thermodynamic and electrical properties stability. Even at SiO_2 layer cutting down to 13 Å MOSFET operates rather successful by [1]. However, at small thicknesses, there exist such undesirable effects as impurity penetration, especially boron from the high doped polysilicon gate. The problems of reliability stable and operation of transistor as well as undesirable leakage currents also appear. For example, in MOSFET with SiO_2 thickness of 3.5 nm at the gate voltage of 1 V the leakage currents are 10^{-12} A/cm^2 and at the thickness 1.5 nm the leakage currents increase by 13 orders and reach 10 A/cm^2 [3]. For the normal operation of microprocessors and fast growing market of mobile phones and portable computers, there is strong demand to decrease the leakage current up to ~10^{-3}A/cm^2 [1]. The problem solution of gate capacity keeping without the gate voltage increase can be provided by SiO_2 layer change for dielectric having a higher value of the dielectric permittivity ε and higher breakdown voltage. Certainly, this new dielectric should be compatible with silicon technology to form the high quality interface with silicon, to be thermodynamic and structurally stable and technologically reproducible. Nowadays, all over world the investigations aimed at the change of the silicon oxide are carried out. The favorites of investigations are [1]: Ta_2O_5, $SrTiO_3$, Al_2O_3, $Ba_xSr_{1-x}TiO_3$, $Pb_xZr_{1-x}TiO_3$, Y_2O_3, La_2O_3, Pr_2O_3, TiO_2, ZrO_2, and HfO_2. But for all these materials, there is the problem of high quality interface with silicon formation. For the most cases, the density of trap states is ~10^{12} cm^{-2} eV^{-1}.

One from perspective materials with the big ε value is cerium dioxide CeO_2 that can be deposited by different methods [4-9]. E.g., in the work [6] it was obtained the perfect quality of the interface CeO_2/Si with the state density $6.8\cdot10^{10}$ eV^{-1}cm^{-2} after annealing the deposited film

© 2004, V. Lashkaryov Institute of Semiconductor Physics, National Academy of Sciences of Ukraine

in oxygen at temperature 500°C. Cerium dioxide was employed as a gate insulator for an enhancement-type n-channel metal-oxide semiconductor (MOS) transistor [10]. With CeO_2 gate MOS device yielded an interface charge of $1.5 \cdot 10^{10}$ Coul/cm^2 with threshold voltage of 0.3 V. Because the threshold voltage was positive the CeO_2 application rejected the problem of an additional processing step for charge reduction that exist for SiO_2 dioxide. In the work [11], CeO_2 film in the structure CeO_2/Ge in MOSFET promoted the elimination of the native germanium oxide formation, which is an important result opposite to the case of usual uncontrolled native substrate oxide growth.

In this work, we propose the results of investigation of optical properties inherent to dielectric layers based on CeO_2, namely: CeO_2, WO_3, WO_3+CeO_2, CeO_2+Dy_2O_3 with the aim to get dielectric possessing a high ε value. This class of materials was chosen as based on previous investigations of electrical properties that showed the possibility to get the high quality interface with silicon, where the density of surface traps was $\sim 10^{10}$ cm^{-2}eV^{-1} [12] and breakdown voltage reached 3 – $3.2 \cdot 10^6$ V/cm. The obtained result of high quality interface is explained by small lattice mismatches between CeO_2 and Si. It is known [3] that binary oxide CeO_2 has the high value of dielectric permittivity $\varepsilon = 18 \ldots 26$ that allows to hope on increase in CeO_2 films in comparison with silicon dioxide. Though it is known [1] that properties of thin films materials strongly differ from properties of volume materials and under thickness reduction the ε value is also decreased. The incorporation of rare earth element Dy into the CeO_2 film was fulfilled because Dy promotes the electric properties stabilization that is very important start to solve from the put problem for application of new dielectric material [1].

The optical properties were investigated by the methods of infrared (IR), Raman spectroscopy and ellipsometry. Infrared reflection spectra were measured at 20° angle of incidence using a Bruker IFS 66 Fourier Transform Infrared Spectrometer based on the Michelson Interferometer. Raman spectra were excited using Kr^+ Innova – 300 laser. Measurements were made using the, wave length 647.1 nm, resolution achieved 2.5 cm^{-1}, radiation power was 15 mW. It was used nonpolarized radiation. The spectral analysis was performed by a Dilor XY 800 triple monochromator equipped with a Peltier cooled Wright CCD detector. Spectroscopic ellipsometry measurements were performed using a variable angle spectroscopic ellipsometer (VASE from J.A. Woollam Co., Inc.) equipped with a Xe-lamp source, single chamber monochromator, continuously rotating analyser and auto-retarder. The ellipsometric angles Ψ and Δ were determined in the spectral range 0.8 to 5 eV at 65°, 70° and 75° angles of incidence. For data evaluation, the measured samples were described by a model taking into consideration the silicon substrate with an oxide layer on top, covered by the film containing CeO_2 and an additional top layer consisting of 50% film material and 50% void material for modeling the surface roughness. For the silicon and SiO_2, optical constants data base values were used. From the measured data, the thickness of the SiO_2 film, thickness and roughness of CeO_2 containing films and their optical constants were determined.

The standard X-ray diffractometr (Model DMAX-B, Rigaku, Tokyo, Japan) was used to determine the crystalline phases present in the samples. To identify compounds, we used JCPDF card files to match peak positions of possible CeO_2, WO_3 oxides.

2. Technology of deposition

All the experiments were performed using commercially available *p*-Si (100) wafers (≈ 440 μm) with a resistance of 4–10 Ω·cm, oxidized at temperatures about 940°C at atmospheric pressure in dry O_2. Thin evaporated layers of CeO_2, WO_3, WO_3+CeO_2, CeO_2+Dy_2O_3 were deposited by technology of flash evaporation from powder original materials onto the oxidized Si substrate. Before the deposition process, the substrates were cleaned in the solution:

1part H_2O_2 + 1 part NH_4OH + 4 part H_2O

and then washed in deionised water for 10 minutes. These Si substrates with different thicknesses of SiO_2 were used to check SiO_2 thickness influence on properties of deposited films. The powder of CeO_2, WO_3 and couple WO_3+CeO_2 (the powder concentration of CeO_2 was 10, 15 and 20 % of the common powder amount), CeO_2+Dy_2O_3 (concentration Dy_2O_3 was 10, 15, 20% of the common powder amount) were used as material sources. The substrate temperature during the evaporation was 170…180°C. The chamber pressure was 10^{-5} Pa. The light-doses of evaporated materials reached the tungsten filament with definite frequency supplied for the keeping of stoichiometric composition of double systems, evaporated and deposited onto the substrate with SiO_2. SiO_2 layers were used because the interface SiO_2/Si has the highest quality. However, the SiO_2 presence leads to reduction of the equivalent thickness of CeO_2+SiO_2 structure in comparison with the equivalent thickness of CeO_2 film.

3. Investigation of films chemical content

The results of X-ray diffraction demonstrate that CeO_2 films have sharp peaks of cerium dioxide in crystalline phase (Fig. 1). As is known [1], the polycrystalline films have higher ε than the amorphous ones. However, the leakage current in polycrystalline films is also higher in comparison with that of the amorphous ones. Amorphous films are more homogeneous and better reproducible. Thus, it is more preferable to get amorphous films as gate dielectric in MOSFET, though the dependence on film structure and transistor operation is not studied well yet [1]. The task to prepare amorphous films based on CeO_2 was solved by deposition of complex films WO_3+CeO_2. The films of pure WO_3 possess an amorphous structure,

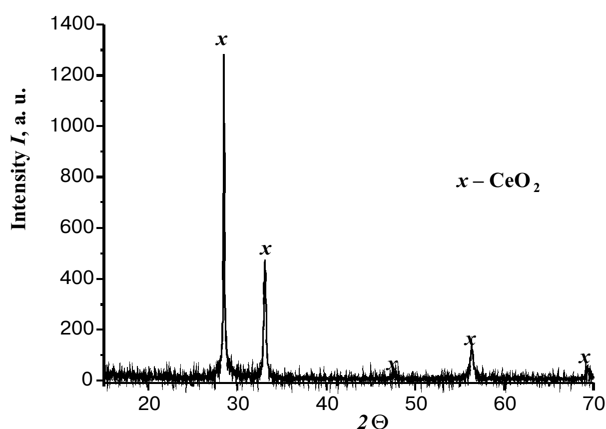

Fig. 1. X-ray diffraction spectrum of CeO_2 film.

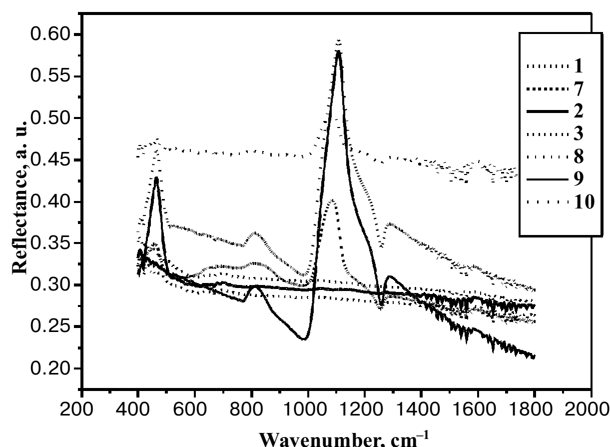

Fig. 2. IR-spectrums of the films: *1, 2, 3* – CeO_2, *7* – WO_3+20% CeO_2, *8* – CeO_2+15% Dy_2O_3, *9, 10* – CeO_2+20% Dy_2O_3.

as it follows from X-ray diffraction results. It was obtained that after CeO_2 introduction the resulting complex films WO_3 + CeO_2 also possess the amorphous structure with impregnation of polycrystalline particles of CeO_2.

4. Results of Raman spectroscopy

All Raman spectra of investigated materials have the same character and show neither the presence of peak at the wavelength 466 cm^{-1} typical for nanocrystalline CeO_2 films [13] no others peaks. The only peak of silicon was present. From the obtained results, it can be concluded that the energy of exciting radiation at the wavelength 647.1 nm is not enough to excite vibrations, and hence studied materials have the wide bandgap.

5. Results of infrared spectroscopy investigation

From the IR reflection spectra of the researched materials (Fig. 2),it is seen that the deposited films have different thicknesses and deposited on the substrates with different thicknesses of native oxide. The samples with CeO_2 films (1, 2, 3) do not show the presence of Si–O oxides in the films. Their spectral behaviour indicates that only a very thin native oxide layer is on the top of substrates. There were not the peaks indicative of the presence of vibrations inherent to SiH_x and Si–OH bonds and to water absorbed as free. The spectra of the samples with complex films WO_3+20%CeO_2 (7), CeO_2+20%Dy_2O_3 (9,10) and CeO_2+15% Dy_2O_3 (8) show the presence of thick native oxide on the substrates (462 nm). The strong feature at 1100 cm^{-1} (sample WO_3+20% CeO_2, CeO_2+15% Dy_2O_3 and CeO_2+20% Dy_2O_3) and two weaker features at 466 cm^{-1} and 820 cm^{-1} are characteristic for SiO_2. The weak peaks at 700 and 1600 cm^{-1} possibly concern with vibration modes of CeO_2 element.

The IR spectra of complex films WO_3+CeO_2 (5,6,7) at different cerium dioxide concentrations (10, 15, 20%) and pure WO_3 (4) film are presented in Fig. 3. It is seen that CeO_2 introduction into WO_3 film does not essentially change the original dependence character. Only for the sample with CeO_2 content 10 %, the peaks near 1600 cm^{-1} become more intensive.

6. Results of ellipsometry

The film thickness and optical constants are determined by the ellipsometry method. There were used several simulation models applying point-by-point fit, model description of optical constants, and Kramers-Kronig consistent. It is obtained that the film thickness varies in the range 72–154 nm at the surface roughness of 5–12 nm (Table 1). SiO_2 thickness is 6 ± 1 to 464 ± 1 nm, which is in a good agreement with results of IR spectroscopy.

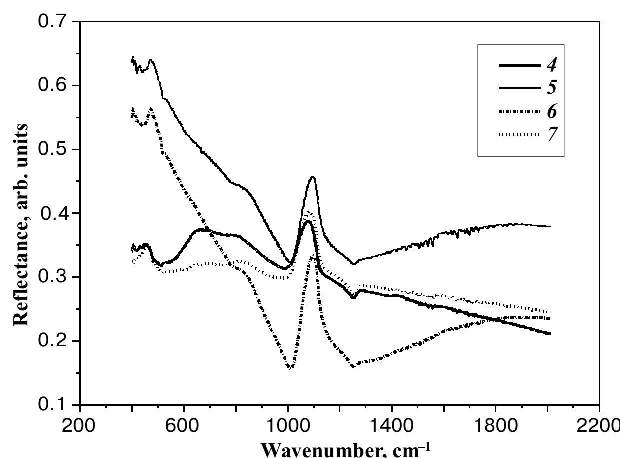

Fig. 3. IR-spectrums of the films: *4* – WO_3, *5* – WO_3+10% CeO_2, *6* – WO_3+15% CeO_2, *7* – WO_3+20% CeO_2.

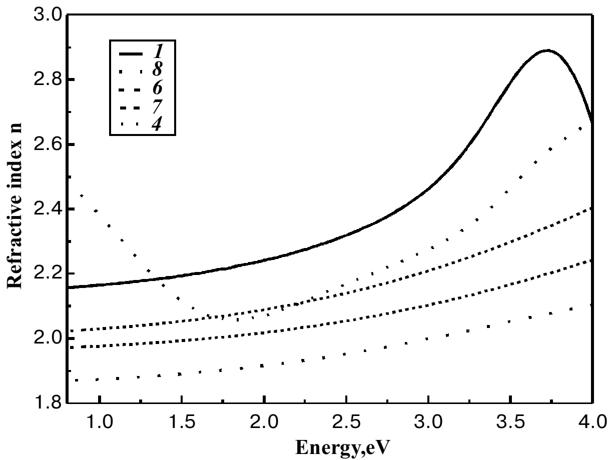

Fig. 4. Refractive coefficient dependence on photon energy for the films: *1* – CeO_2, *4* – WO_3, *6* – WO_3+15% CeO_2, *7* – WO_3+20% CeO_2, *8* – CeO_2+15% Dy_2O_3.

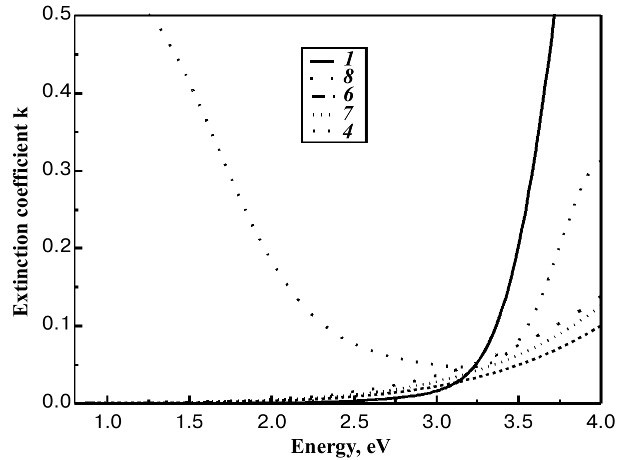

Fig. 5. Extinction coefficient dependence on photon energy for the films: *1* – CeO_2, *4* – WO_3, *6* – WO_3+15% CeO_2, *7* – WO_3+20% CeO_2, *8* – CeO_2+15% Dy_2O_3.

Under the usage of different simulation models for optical constant calculations it was obtained that the point-by-point approach gives more details for the character of refraction and extinction coefficients behavior having non-monotonic character with absorption spectrum broadening near the absorption edge. However, at this approach received is a plenty of noise signals, and parameters accuracy is 3–10 % for different films because of big number of unknowns. The results of optical constants evaluation by the point-by-point and Kramers-Kronig approaches are presented in Figs 4, 5 and Table 2. From Fig. 4 (Kramers-Kronig approach), it is seen that CeO_2 refraction coefficient varies from 2.17 to 2.85, which is a little bit higher than literature data (1.85–2.4) [14] and our previous results (2.2–2.4) [15]. This change of optical constants of complex WO_3+CeO_2 films do not depend on the cerium content in the film and dioxide silicon thickness.

On the base of obtained results of the point-by-point approach, it is plotted the dependence of wide bandgap E_g on absorption coefficient $\alpha^{1/2}$ presented in Fig. 6 (*a–e*). WO_3 film has the biggest value ε =5.76 obtained by the

Table 1. The thickness of silicon dioxide and deposited films obtained by ellipsometry method.

Sample	Thickness, nm			Thickness non-uniformity
	SiO_2	Film	Surface roughness	
WO_3+15%CeO_2, (6)	143 ± 1	72 ± 1	5 ± 1	<5
WO_3+20%CeO_2, (7)	144 ± 1	102 ± 1	6 ± 1	<4
CeO_2+20%Dy_2O_3, (9)	464 ± 1	35 ± 2	7 ± 1	<3
CeO_2, (1)	6 ± 1	154 ± 1	12 ± 1	<14
WO_3, (4)	138 ± 2	116 ± 1	9 ± 1	<5

Table 2. The films optical constants and energy band gaps.

Sample	n_{min}, $h\nu$ = 1.0 eV		$\varepsilon = n^2 - k^2$		E_g, eV
	Point-by-point fit	Kramers-Kronig model	Point-by-point fit	Kramers-Kronig model	Point-by-point fit
CeO_2	2.08	2.17	4.32	4.7	3.15
WO_3	2.14	2.4	4.55	5.76	3.37
WO_3+CeO_2 (15%)	2.0	1.98	4.0	3.92	2.8
WO_3+CeO_2 (20%)	2.05	2.04	4.2	4.16	3.0
CeO_2+Dy_2O_3 (20%)	1.89	1.89	3.57	3.57	2.3

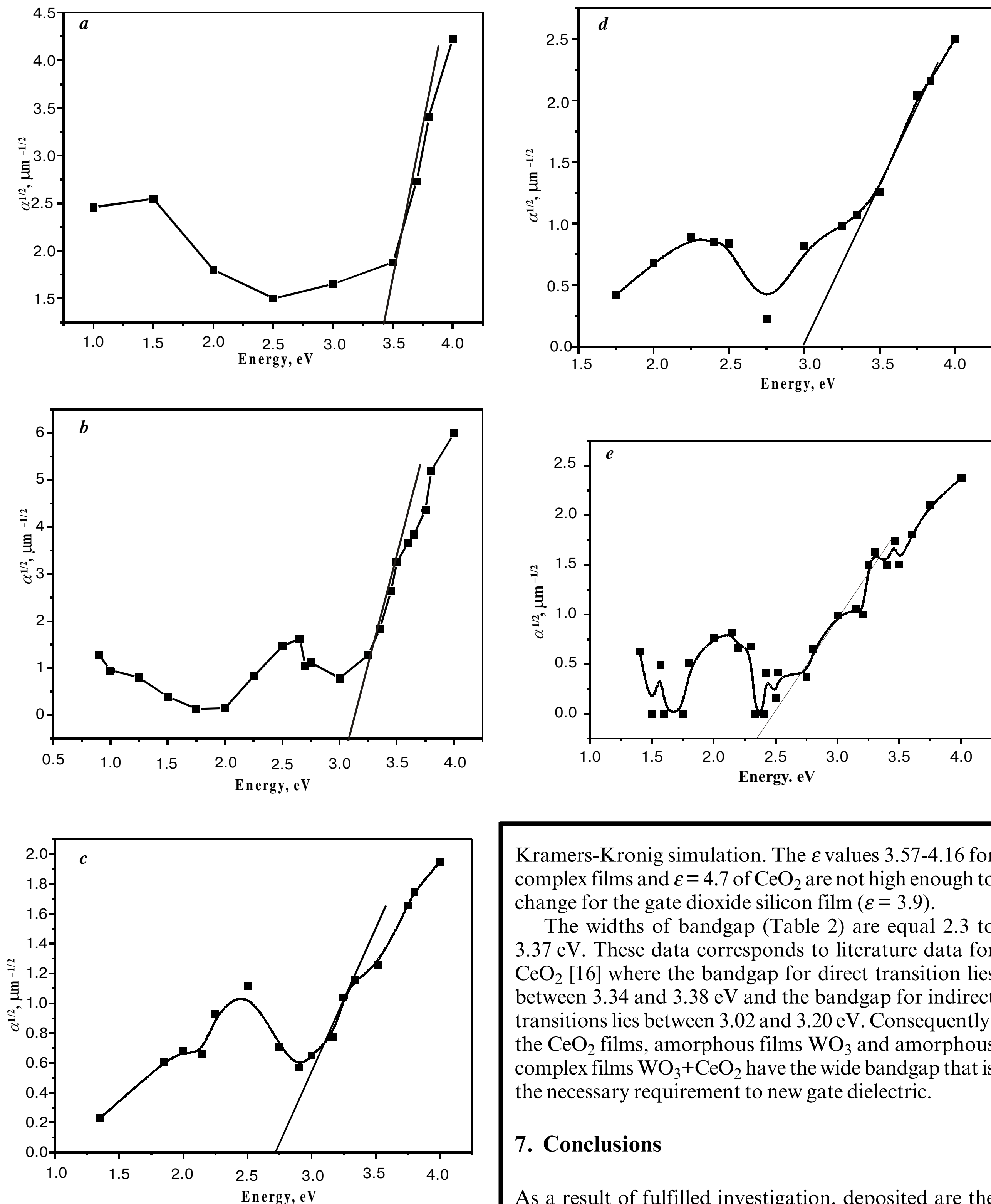

Fig. 6. Plot of the absorption coefficient $\alpha^{1/2}$ versus photon energy for different films: *a* – WO_3; *b* – CeO_2, *c* – WO_3+CeO_2 (15%); *d* – WO_3+CeO_2 (20%); *e* – CeO_2+Dy_2O_3 (20%). The point of crossing of straight line and energy axis notes the energy band gap value.

Kramers-Kronig simulation. The ε values 3.57-4.16 for complex films and $\varepsilon = 4.7$ of CeO_2 are not high enough to change for the gate dioxide silicon film ($\varepsilon = 3.9$).

The widths of bandgap (Table 2) are equal 2.3 to 3.37 eV. These data corresponds to literature data for CeO_2 [16] where the bandgap for direct transition lies between 3.34 and 3.38 eV and the bandgap for indirect transitions lies between 3.02 and 3.20 eV. Consequently, the CeO_2 films, amorphous films WO_3 and amorphous complex films WO_3+CeO_2 have the wide bandgap that is the necessary requirement to new gate dielectric.

7. Conclusions

As a result of fulfilled investigation, deposited are the polycrystalline thin films of CeO_2, amorphous films WO_3, amorphous complex films WO_3+CeO_2 and CeO_2+Dy_2O_3. For the first time, the optical characteristics of complex films WO_3+CeO_2 and CeO_2+Dy2O_3 are presented. The IR results are indicative of SiO_2 presence in the films except for CeO_2. Water in the films is not found. The refraction coefficient (n = 1.85–2.85) for CeO_2 films is a little bit higher than that presented in literature data.

The n value of complex films is not more than 2.37. The calculated ε =3.57–4.16 of complex films and ε = 4.7 of CeO_2 do not allow to change for the gate dioxide silicon film. The deposited new films CeO_2, WO_3 and WO_3+CeO_2 have wide bandgap E_g = 2.8–3.37 eV.

To increase the dielectric permittivity ε, it is possible to introduce some changes into the technological process of film evaporation. For example, to carry out the evaporation in the environment of oxygen or nitrogen (NH_3, N_2) with annealing treatment that, as is known [6,17,18], leads to film defect reduction.

Acknowledgment

The author thanks A.N. Shmyryeva (NTUU "KPI") for the given samples and long time heading the authores work, V.G. Litovchenko for the consultation under results processing, Marion Friedrich and D.R.T. Zahn for the possibility to work in their laboratory of semiconductor physics in TU-Chemnitz, Germany. This work was financially supported by the grant from Ministry of Education of Saxon, Germany.

References

1. G.D. Wilk, R.M. Wallance, and J.M. Anthony, High-k gate dielectrics: Current status and material properties considerations // *J. Appl. Phys.*, **89**(10), pp. 5243-5275 (2001).
2. Int. Technology Roadmap for Semiconductors, http://www.public.itrs.net.
3. Rainer Waser (editor), Silicon MOSFETs-Novel Materials and Alternative Concepts, Chap.13 in *Nanoelectronics and Information Technology*, Eds. Rainer Waser, pp. 361-385, Wiley-VCH, Weinheim, Germany, (2003).
4. T. Inoue, Y. Yamamoto, and M. Satoh, Low temperature epitaxial growth of CeO_2 (110) layers on Si (100) using electron-beam assisted evaporation // *Thin Solid Films*, **343-344**, pp. 594-597 (1999).
5. L. Kim, J. Kim, D. Jung, Ch.–Y. Park, Ch.–W. Yang, and Y. Roh, Effect of deposition parameters on the crystallinity of CeO_2 thin films deposited on Si (100) substrates by r.f.–magnetron sputtering // *Thin Solid Films*, **360**, pp. 154-158 (2000).
6. H.W. Song, Ch. S. Lee, D.G. Kim, and K. No, Characterization of CeO_2 thin films as insulator of metall ferroelectric insulator semiconductor (MFIS) structures // *Thin Solid Films*, **368**, pp. 61-66 (2000).
7. S. Gnanarajan, and N. Sawides, Evolution of texture of CeO_2 thin film buffer layers prepared by ion-assisted deposition // *Thin Solid Films*, **350**, pp. 124-129 (1999).
8. B. Elidrissi, A. Addou, M. Regragui, C. Monty, A. Bougrine, and A. Kachouane, Structural and optical properties of CeO_2 thin films prepared by spray pyrolysis // *Thin Solid Films*, **379**, pp. 23-27 (2000).
9. B. Hirschauer, G. Chiaia, M. Goethelid, and U.O. Karlsson, Studies of highly oriented CeO_2 films grown on Si (111) by pulsed laser deposition // *Thin Solid Films*, **348**, pp. 3-7 (1999).
10. A.G. Frangoul, K.B. Sundaram, and P.F. Wahid, The fabrication of metal-oxide-semiconductors using cerium dioxide as a gate oxide material // *J. Vac. Sci. Techol. B*, **9**(1), pp.181-183 (1999).
11. D.P. Norton, J.D. Budai, and M.F. Chisholm, Hydrogen-assisted pulsed-laser deposition of (001) CeO_2 on (001) Ge // *Appl. Phys. Letters,* **76**(13), pp. 1677-1679 (2000).
12. A.N. Shmyryeva, V.V. Naumov, V.A. Kochelap, and T.V. Semikina, Inversion Solar Cell based on Silicon Structure with Cerium Oxide // *World Renewable Energy Congress* VII, 29 June-5 July, 2002, Cologne, Germany.
13. I. Kosacki, V. Petrovsky, and H.U. Anderson, Raman spectroscopy of nanocrystalline ceria and zirkonia thin films // *J. Am. Ceram. Soc.*, **85**(11), pp. 2646-2650 (2002).
14. K.B. Sundaram, P.F. Wahid, and P.J. Sisk, Characterization and optimization of cerium dioxide films deposited by r.f. magnetron sputtering // *Thin Solid Films*, **221**, pp. 13-16 (1992).
15. O.V. Fursenko, T.V. Semikina, and A.N. Shmyryeva, Fabrication and ellipsometric investigation of thin films of rare-earth oxides // *Solid State Phenomena*, **63-64**, pp. 341-346 (1998).
16. K.B. Sundaram, and P. Wahid, Optical absorption in cerium dioxide thin films // *Physica Status Solidi (b)*, **161,** K63-K66 (1990).
17. Seok-Woo Nam, Jung-Ho Yoo, Suheun Nam, Dae-Hong Ko, Cheol-Woong Yang, and Ja-Hum Ku, Characteristics of ZrO_2 films with Al and Pt gate electrodes // *J. of The Electrochem. Soc.*, **150**(12), G849-G853 (2003).
18. R. J. Carter, E. Cartier, A. Kerber, L. Pantisano, T. Schram, S. De Gendt, and M. Heyns, passivation and interface state density of SiO_2/HfO_2-based/polycrystalline-Si gate stacks // *Appl. Phys. Letters*, **83**(3), pp.533-535 (2003).